

ポリ 3 ヘキシルチオヘン薄膜の構造と移動度 Structure-mobility Relationship in Poly(3-hexylthiophene) Films

Shizuyasu OCHIAI †, Xin Wang †, and Kenzo KOJIMA †
落合鎮康、汪 昕、小嶋憲三

Abstract: Low-cost organic field-effect transistors (OFETs) were fabricated with soluble and crosslinkable poly(4-vinylphenol) (PVP) as the gate insulator and poly(3-hexylthiophene) (P3HT) as the active semiconductor which was cast by spin-coating or drop-casting method. The substrate was glass or poly(ethylene naphthalate) (PEN). As a comparison, OFETs with vacuum deposited pentacene film and polycarbonate (PC) gate insulator were also fabricated and investigated. We get the following conclusion. Aggregation states and charge transfer mechanisms in the P3HT films were studied in OFETs. Both regioregular and regiorandom P3HT (RRa-P3HT) were studied and also the oligomer acenes of pentacene. Pentacene films were deposited by the physical vapor deposition (PVD) method on the gate insulator of PC. RRa-P3HT films showed mobilities one or two orders lower than those of RR-P3HT films because they were amorphous in both spin-coated and drop-cast films. Experimental results also revealed a correlation between the mobility and the aggregation states that the larger aggregate size and number can result in the higher mobility. Pentacene films (in herringbone structure) displayed mobilities about two orders higher than RR-P3HT (in lamellar structure), because it formed polycrystalline films with crystal size being much larger than those in RR-P3HT semicrystalline films. For RR-P3HT films, aggregation with the π - π stacking interaction was found to assist the planarization of the polymer backbones, however, the alkyl side-chain interactions could result in chain folding within one polymer, and hence decrease the crystallinity and mobility greatly. Multiple π - π^* absorption peaks for RR-P3HT thin films were ascribed to the vibronic progression with the in-plane ring breathing mode assisted by polymer aggregation but not to the typical Davydov splitting; and this explanation coincide well with the relatively poor crystallinities and low mobilities in semicrystalline P3HT thin films. These results imply that there are still many spaces to increase the mobility of π -conjugated polymer films if larger π - π stacked crystal size can be obtained. The performances of the OFETs can be further improved by optimizing the structure and morphology of organic semiconductor film, the properties of the gate insulator layer, and the configuration of the OFETs. For real applications of all-polymer transistors, their stability should also be enhanced. Insertion of an isolation layer or a vacuum package is recommended to prevent ambient humidity, oxygen, and unintended doping.

1. Introduction

Functional properties of organic molecules and polymers continue to attract enormous attention in contemporary chemistry and physics. Over the past two decades, there has been great interest in organic semiconductors, driven by their potential use in light-emitting diodes, photovoltaic devices, organic integrated circuits, and low-cost disposable electronics applications [1-5]. Using π -conjugated organic molecules or polymers as active materials has introduced novel concepts in device designs. In particular, there has been special interest in solution processable π -conjugated organic molecules from small molecules to oligomers and polymers, due to their flexible chemical tunability, low-temperature processing, large area coverage, and light-weight low-cost applications. They are suitable to use wet coating techniques including spin-coating, drop-casting, dip-coating, spray-coating, screen-printing and ink-jet printing; and eliminating the need for many of the major semiconductor-manufacturing cost points, including lithography, physical vapor deposition (PVD) and chemical vapor deposition (CVD), plasma etching, and the high waste management costs. Comparing with small organic molecules, polymers show unique charge transfer characteristics in chains and usually superior mechanical and thermal stabilities. Amazingly, the conductivity of polymers can be tuned from insulator to good conductor by chemical manipulation of the

polymer backbone, by the nature of the dopant, by the degree of doping, and by blending with other polymers; they have potential applications at almost all levels of microelectronics and towards the goal of all-polymer electronics [5-7].

Organic field-effect transistors (OFETs) are among the most attractive constituent elements for high-density organic devices. Recently, OFETs have been used as integrated circuits [8], chemical sensors [9], and switching devices for active-matrix flat-panel display (AMFPD) [10, 11]. Unfortunately, the performances of OFETs usually cannot rival the performances of field-effect transistors (FETs) based on inorganic semiconductors such as Si and Ge, with the mobilities being several orders of magnitude lower. Great deals of efforts were made to improve the mobility and performances of OFETs. Different kinds of newly synthesized organic semiconductors were tried; and at present, some oligomers (for example, oligoacene and oligothiophene) and polymers (for example, poly(3-alkylthiophenes) (P3ATs)) show high mobilities which are getting closer to those of inorganic materials. Comparing with small organic molecules, polymers show unique charge transfer characteristics in chains and usually superior mechanical and thermal stabilities. One of the keys to improving the mobility is to develop an understanding of the relationship between organic thin-film structure/morphology and charge transport. At low temperatures, coherent band-like transport of delocalized carriers was found in single crystals of pentacene, tetracene, and other acenes [12-14]. Even at room temperature, mobility as high as to $\sim 15 \text{ cm}^2 \text{V}^{-1} \text{s}^{-1}$ was found for rubrene single crystals [15].

† 愛知工業大学 工学部 電気学科 (豊田市)

Band-like transport was also shown along the crystal directions with high π - π^* orbital overlap in single crystals of oligo-thiophenes [16]. Band transport is not applicable to disordered organic semiconductors, where carrier transport takes place by hopping between localized states and carriers are scattered at every step. The boundary between band transport and hopping is defined by materials having room-temperature mobilities of the order of $1 \text{ cm}^2 \text{ V}^{-1} \text{ s}^{-1}$ [17, 18]. For π -conjugated oligomers and polymers, it is also generally accepted that charges can transport along the oligomer or polymer chains in their doped state, by means of polarons or bi-polarons. It is believed that longer chain is more propitious to the intrachain charge transport if the coplanarity is guaranteed in the polymer. However, it is very hard to get high-purity, defect-free, and monodisperse polymers, and crystallization of polymers is still a big challenge for chemists. Some polymers can form semicrystalline or polycrystalline structures in solid states, however, their structure-mobility relationships are not very clear yet till now.

The choice of gate dielectrics for OFETs is very important. It is highly desirable that the SiO_2 insulator is substituted with an organic dielectric to realize low-cost and large-area all-organic electronics. Among various polymer insulators, poly (4-vinylphenol) (PVP) is promising candidates of good gate dielectric which can be easily dissolved in some solvents and can also be chemically crosslinked. Because of the phenol structure in the side chains, PVP is considered to possess better resistance against moisture absorption. Polycarbonate (PC) has been widely used in the modern industry due to its wonderful physical properties such as considerable mechanical strength, high resistivity, good optical transparency and effective heat-resistance. It can be dissolved in many kinds of organic solvents and easily made into thin films. We also tried PC as gate insulator for pentacene OFETs.

2. Experimental Details

2.1 Crosslinking of PVP thin film

The mechanism of heat-induced crosslinking for the PVP sample is shown in Fig. 1. Film thicknesses were measured using a surface profile measuring system (Dektak IIA, Sloan Tech.).

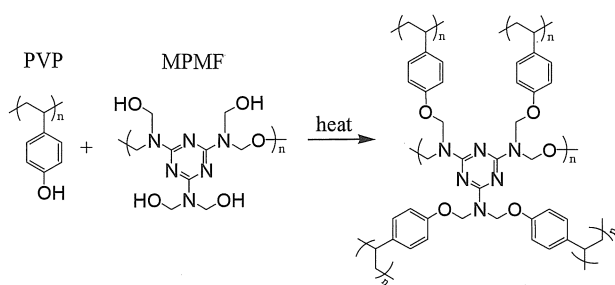


Fig. 1. Mechanism for heat-induced crosslinking of PVP with MPMF as crosslinking agent.

2.2 Fabrication of OFETs

The P3HT OFETs were fabricated with the “bottom-gate” and “top-contact” configuration on a cleaned glass substrate (Matsunami Glass) or PEN, as shown in Fig. 2 (a), the gate insulator was crosslinkable PVP. The pentacene OFETs were fabricated with the “bottom-gate” and “bottom-contact” configuration on a cleaned glass substrate or

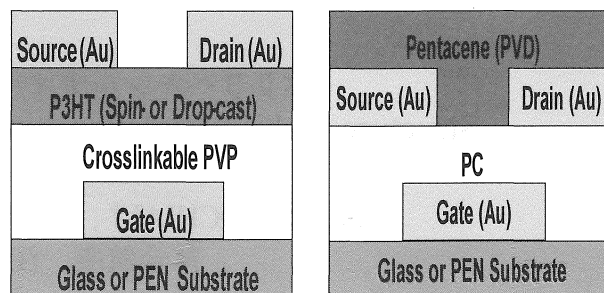


Fig. 2 (a) “Bottom-gate” and “Top-contact” configuration for P3HT OFETs; (b) “Bottom-gate” and “Bottom-contact” configuration for pentacene OFETs.

PEN as shown in Fig. 2 (b), the gate insulator was PC (FE-2000; Mitsubishi Engineering-Plastics). The replacement of glass substrates by the PEN substrates can realize the flexible all-polymer OFETs. Strictly speaking, for all-polymer OFETs, the electrodes should also be replaced by polymer electrodes, for example, poly (3,4-ethylenedioxythiophene) : poly(styrene sulfonic acid) (PEDOT : PSS) or polyaniline (PANI). Here, we use gold electrodes and sometimes glass substrates to investigate the performances of OFETs under different fabrication conditions.

RR-P3HT, synthesized by Rieke method, was purchased from Aldrich Chemical Co. with the regioregularity $> 98.5\%$ and a nominal weight-average molecular weight M_w of ~ 87000 from the supplier. However, the measured M_w could be somehow lower as ~ 52000 [19]. Assuming the M_w to be ~ 70000 , we can estimate the contour length of our RR-P3HT to be ~ 160 nm. Structure, morphology and aggregation states of RR-P3HT films were controlled by spin-coating at different spin speeds and drop-casting from chloroform solutions. Spin-coating was carried out at 2000 rpm and 4000 rpm for 20 s with a concentration of 0.2 wt%. Drop-cast films were cast with a 10 μl drop from a dilute chloroform solution of 0.05 wt%, and were enclosed in a Petri dish to increase the evaporation time. As comparison, regiorandom P3HT (RRa-P3HT; Aldrich) and pentacene (Aldrich) were also used to fabricate OFETs. The fabrication procedure of RRa-P3HT OFET was from the solution in CHCl_3 and similar to that of RR-P3HT. Pentacene films were vacuum deposited onto PC gate insulator by PVD technique. It was found that on PVP gate insulator (non-crosslinked or crosslinked) the vacuum deposited pentacene films were not uniform with many bubble-like defects, so we choose PC as gate insulator for pentacene OFETs and the pentacene films were optically smooth with high quality. Gold gate (G), source (S) and drain (D) electrodes were deposited with controlled evaporation rates under a vacuum of 3×10^{-6} Torr. High-speed deposition of S and D might destroy the organic thin films and make a short circuit with the G electrode; thus, an evaporation speed ≤ 0.05 nm/s was used for S and D. Electrode thickness ranged from 20 to 50 nm depending on the evaporation time. A rectangular mask (with channel wide W of 1000 μm and length L of 20 μm) and a twenty-interdigitated mask (with total W of 19 mm and L of 50 μm when neglecting the fringing fields) for S and D electrodes were used. The thickness for spin-coated P3HT (RR or RRa) film at 2000 and 4000 rpm was ~ 35 nm and ~ 25 nm, respectively. For drop-cast film, it is not smooth with an averaged thickness ~ 90 nm. The typical thickness for vacuum deposited pentacene film was about 110 nm. Film structures, morphologies and aggregation

states were characterized using UV-visible absorption spectra (UV-2450, Shimadzu), tapping-mode AFM (NV-2000, Olympus), and out-of-plane XRD. Peak separation of the P3HT UV-visible absorption spectra was carried out using a commercial software PeakFit v4.12.

3. Results and Discussion

3.1 Performances of OFETs

The mobilities obtained from OFETs with drop-cast RR-P3HT films are one order higher than those with spin-coated films. This can be explained by the difference of film structures and morphologies including the chain alignments, the interconnectivity of the polymer network, and the size of the self-organized microcrystallites [20, 21]. From the results of AFM images and UV-visible absorption spectra, we know that spin-coated RR-P3HT film is isotropic and almost noncrystalline with small and low-density polymer aggregates; but drop-cast film is self-organized into semicrystalline films containing microcrystalline clusters and fibers. By spin coating, the fast solvent evaporation results in random chain alignment and low molecular ordering. By drop casting, the slower rate of solvent evaporation facilitates slower film growth, and leads to better chain alignment, larger single microcrystallite, and higher degree of order. It extends the carrier transportation from within only one single chain (by hopping to another chain) to the whole microcrystallite (because of strong coupling), and the larger crystalline size suppresses the random scattering of carriers at defects or boundaries, and hence enhances the mobility greatly. However, the OFET with drop-cast RR-P3HT film shows inferior saturation characteristics in the output curves and a lower on/off ratio as compared with the spin-coated film. This is probably due to the higher roughness and thickness of the drop-cast film with fiber structures, and hence nonnegligible carrier transportation in bulk of the P3HT film. Roughness causes nondirectional scattering of carriers and usually decreases the OFET performance including the saturation characteristics in the output and the on/off ratio. More experiments are needed to clarify the mechanism. The bulk transportation in thick drop-cast film can be partially proved by the conductance measurements shown in Fig. 3. The current intensities were measured between two electrodes (the same as the S and D electrodes in the OFET) which were deposited onto spin-coated/drop-cast RR-P3HT thin films. Under our conditions, current in the drop-cast film is about ten times of that in the spin-coated one, clearly revealing the higher bulk transportation. From the electrodes' configuration and film thickness, the electrical conductivity σ can be estimated. For the spin-coated film of thickness about 35 nm, we get $\sigma \approx 1.9 \times 10^{-6}$ S/cm. For the drop-cast film, however, we cannot obtain an exact conductivity value because the film is not smooth, and the fiber and non-fiber parts probably possess different conductivities. If we only consider the average thickness of the drop-cast film (~100 nm), we get an average conductivity to be $\sim 6.3 \times 10^{-6}$ S/cm, which is about 3.3 times of that of the spin-coated film. In fact the structure and morphology of the drop-cast RR-P3HT film can be further improved by optimizing the evaporation time, solvent species, and surface modification.

Annealing could also alter the film structure/morphology and hence modified the OFET performance. Annealing of the OFETs was performed in the oven under the protection of nitrogen (at 110°C for half an hour). The mobility for spin coated RR-P3HT film increased from a little to several times after annealing; but for drop cast film it remained almost unchanged or

even decreased sometimes. Both UV-vis absorption spectra and XRD profiles displayed that the characteristic peaks of RR-P3HT microcrystallites started to appear (or became more obvious) after annealing for spin-coated films. It means that, for spin-coated RR-P3HT film, it changed from almost amorphous to containing some semicrystalline islands after annealing. However, for drop-cast films, the UV-vis absorption spectra and XRD profiles remained almost unchanged.

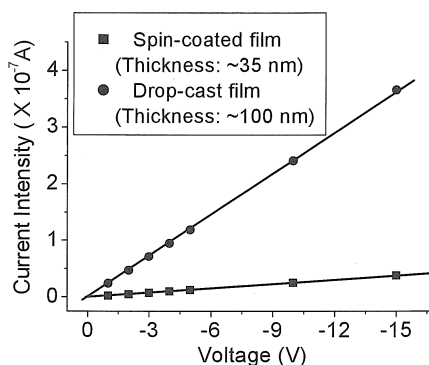


Fig. 3. Conductance measurements of spin-coated and drop-cast RR-P3HT thin films between two electrodes (the same as the S and D electrodes in the OFET) which were deposited onto the films.

Therefore, for drop cast film, the influence of annealing was much less which might come from the fact that it was already in semicrystalline structures. The decrease of mobility might result from unintended oxidation or other degradation of the RR-P3HT thin films under high temperature.

The threshold voltages vary from about -30 to 30 V for these OFETs. Threshold voltage usually depends on the density of carrier trapping states and is sensitive to processing conditions. Even under the same fabrication conditions for the P3HT film, we found that the OFET performance and P3HT mobility could be modified by the properties of dielectric, contact resistance between electrodes and organic films, OFET architecture and other experimental conditions. But, the mechanisms are not very clear yet.

Table 1 summarizes the mobilities of the OFETs on PEN substrate with crosslinked PVP gate insulator and spin-coated (at spin speed of 4000 rpm and 2000 rpm) or drop-cast RR-P3HT active layer. Fig. 4 shows the output and transfer curves of an all-polymer OFET with drop-cast RR-P3HT active layer and crosslinked PVP gate insulator on a PEN substrate. It displayed an excellent saturation

RR-P3HT layer	Spin at 4000 rpm	Spin at 2000 rpm	Drop-cast
Gate Insulator (Crosslinked)	PVP	PVP	PVP
μ ($\text{cm}^2/\text{V}\cdot\text{s}$)	$\sim 4.0 \times 10^{-4}$	$\sim 6.0 \times 10^{-4}$	$\sim 2.0 \times 10^{-2}$

Table 1. Mobilities of the OFETs on PEN substrates with crosslinked PVP gate insulator and spin-coated (at different spin speed of 4000 rpm and 2000 rpm) or drop-cast RR-P3HT active layer.

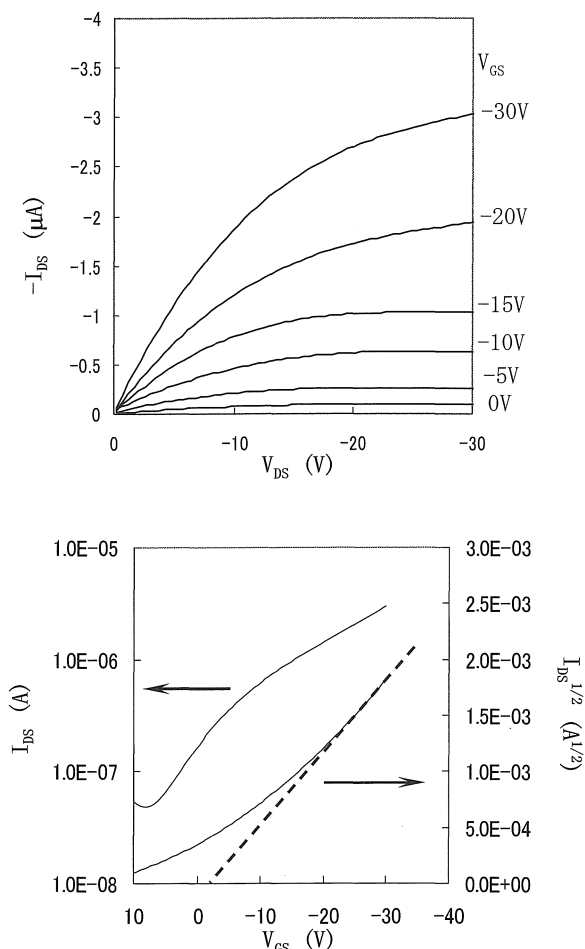


Fig. 4 Output and transfer curves of an all-polymer OFET with drop-cast RR-P3HT active layer and crosslinked PVP gate insulator on a PEN substrate.

property in the output curve. From the saturation region in transfer curve, the field-effect mobility was calculated to be $2.0 \times 10^{-2} \text{ cm}^2/\text{Vs}$ and the threshold voltage was only about -2V . The on/off ratio was over 10^3 . This field-effect mobility is about 2 times of the recently reported one with a similar OFET structure on the SiO_2/Si substrate [22].

These results reveal again the difference of polymer alignment and crystalline structure between the drop-cast and the spin-coated P3HT films, and support again the findings that π - π stacking plays an important role in the carrier transport in the two-dimensional active channel [23].

3.2 Structure-mobility relationship in P3HT films

The experimental results above show that mobility of drop cast RR-P3HT is one or two orders higher than that of spin coated ones at 4000 rpm; mobility of spin coated RR-P3HT film at 2000 rpm is several times higher than that of spin coated one at 4000 rpm. As a comparison, the performances of OFETs based on RRA-P3HT were also investigated. Just as what we have expected, RRA-P3HT OFETs show lower mobilities (typically $\sim 5.0 \times 10^{-5} \text{ cm}^2/\text{V}\cdot\text{s}$ for spin-coated RRA-P3HT and $\sim 1.0 \times 10^{-4} \text{ cm}^2/\text{V}\cdot\text{s}$ for drop-cast RRA-P3HT), which are one or two orders lower than those of RR-P3HT. The UV-vis absorption spectra (Fig. 5) reveal that both spin-coated and drop-cast RRA-P3HT thin films are in amorphous structures (no

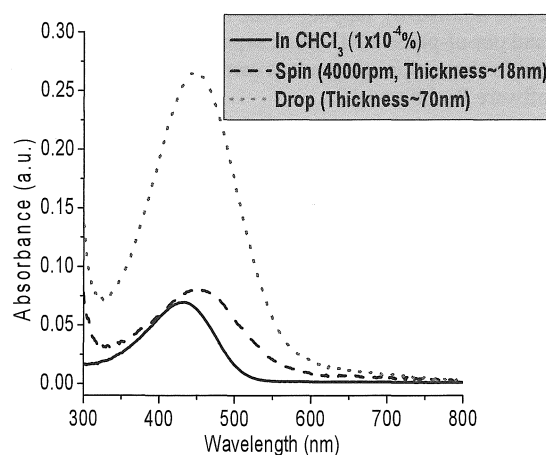


Fig. 5. UV-vis absorption spectra for RRA-P3HT in CHCl_3 solution, and spin-coated and drop-cast films.

shoulder peaks and the position of absorption peak is the same for both spin-coated and drop-cast RRA-P3HT thin films). XRD results also display no diffraction peaks for both spin-coated and drop-cast RRA-P3HT thin films.

It reveals clearly a correlation between the mobility and the aggregation states. Aggregation with lamellar structure show improved mobility and the larger aggregate size and number result in the higher mobility. Big difference of mobility between the drop-cast and the spin-coated RR-P3HT films implies the difference of charge transport mechanism in aggregates and in amorphous areas. But these explanations are not enough to understand the detailed aggregation states and the reasons for the relatively low mobilities in RR-P3HT films as mentioned in the introduction. We have to find more clues. In fact, the origin of the multiple peaks or "fine structure" on the main π - π^* absorption peak in the UV-visible absorption spectra is still a matter of some debate [23-25]. These peaks are only observed in some crystalline conjugated oligomers or regio-regular conjugated polymers in the solid state (or in colloidal aggregates that have molecular packing similar to that of the semicrystalline solids), and only when the size of the side chains allows for close approach of the π -systems on neighboring chains (π - π stacking). The peak separation results for the UV-vis absorption spectra of P3HT films are shown in Fig. 6. At present, there are several competing theories to explain these "fine structures" in the spectra, including the Davydov splitting of the exciton levels due to aggregation by inequivalent sites in the solids [26-28], vibrational coupling or called vibronic progression [29, 30], and exciton band formation by combination of both Davydov splitting and vibrational coupling [24, 25]. Generally speaking, both Davydov splitting and vibrational coupling can exist in the absorption spectra; the relative magnitudes of each of the coupling constants determine the final appearance of the spectra. For RR-P3HT and other regioregular conjugated polymers (for example, poly(3-alkylfuran)s [P3AFs]), investigation into their crystalline structures (aggregation states) with regard to these multiple peaks in the absorption spectra might figure out the specific origin of them and clarify the structure-mobility relationship. Unsubstituted conjugated oligomers and polymers, e.g., pentacene or sexithiophene (6T), tend to crystallize in the "herringbone" or "parquet" pattern wherein the edge of one chain is more or less pointed at the face of a neighboring chain. If the oligomer or polymer chains were substituted with alkyl side groups, then

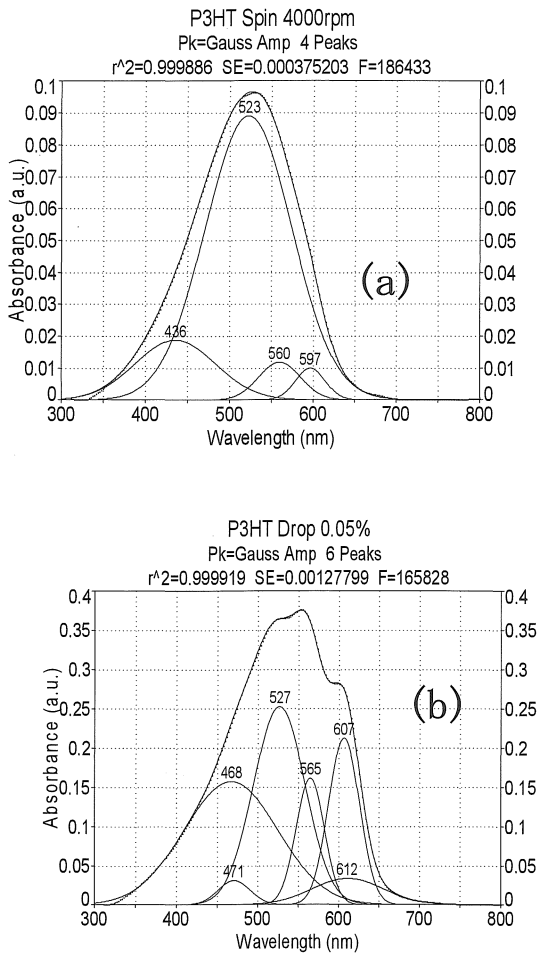


Fig. 6. Peak separation results for the UV-vis absorption spectra of RR-P3HT films: (a) spin at 4000 rpm and (b) drop-cast. Only peaks with FWHM narrower than that of the monomer absorption peak [the peak at 523 nm in (a) or 527 nm in (b)] are considered to be the real absorption bands due to aggregation and vibronic progression. Peak at 612 nm of (b) might be due to long tail scattering at long wavelengths and/or the errors from fitting by ideal Gaussian function. Peaks at around 436 nm in (a) and at around 468 nm in (b) might come from the absorption of amorphous twisted polymers mixing with factors of scattering and errors.

a herringbone-type packing would produce a nanoporous structure. Since the energy tends to be minimized with increasing packing density, porous structures are metastable and tend to collapse to more highly packed structures, e.g., the lamellar structure [34]. This can be also understood by the interactions between the alkyl side chains which “force” the cofacial packing (π - π stacking) of the polymer main chains. The molecular packing is maximal, and the alkyl side chains possess translational symmetry along the chain axis to form a microcrystallite; i.e., the polymers must be “regioregular”.

Figure 7 shows the UV-vis absorption spectrum for pentacene film deposited on PC by PVD on a glass substrate. The peaks in the left circle are from isolated pentacene molecules (pentacene solution) and the peaks in the right circle are new peaks resulted from the aggregation states (pentacene films with microcrystals). Fine peaks of vibronic progression can clearly be found for both pentacene solutions and films.

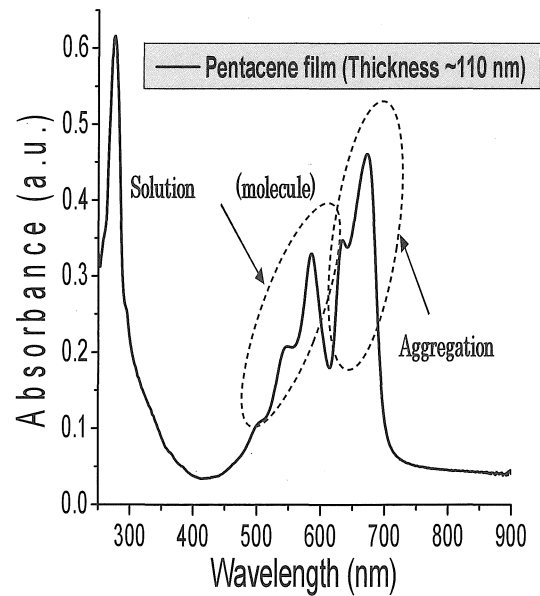


Fig. 7. UV-vis absorption spectrum for pentacene film deposited on PC by PVD on a glass substrate.

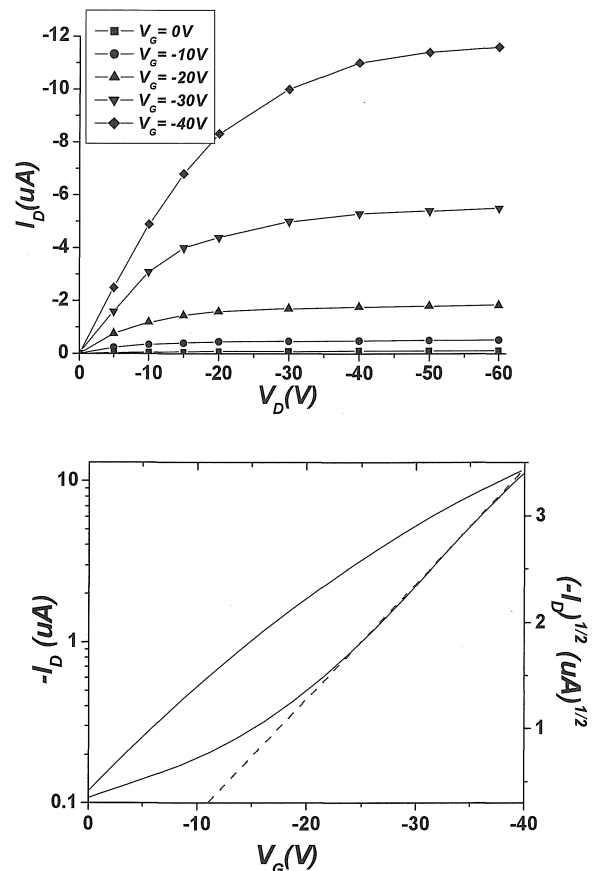


Fig. 8. The output and transfer curves of an OFET with vacuum deposited pentacene and PC gate insulator.

Right shift of the aggregation peaks reveal an aggregation state similar to the J-type aggregation, which is due to the large tilting angle in its herringbone structure.

The output and transfer curves of an OFET with vacuum deposited pentacene and PC gate insulator are displayed in Fig. 8. The mobility is calculated to be about $0.26 \text{ cm}^2/\text{Vs}$. So pentacene shows mobility about one order higher than that of RR-P3HT. In the literature, some substituted oligothiophenes can also display mobilities up to $\sim 1 \text{ cm}^2/\text{Vs}$ [33], which are about one order higher than that of RR-P3HT ($\sim 0.1 \text{ cm}^2/\text{Vs}$). The difference between the mobilities can be understood by the difference between the crystal structure (aggregation state) and microcrystal size. AFM and XRD experiments reveal that pentacene microcrystal size (about 1–2 micron) is much larger than that of RR-P3HT (about 10–20 nm). The lamellar structures have been proved in P3ATs and some other regioregular conjugated polymers by detailed investigation of their crystal structures, for example, XRD patterns. It is well accepted that the π - π stacking leads to H-aggregation. According to Davydov splitting theory, H-aggregation leads to a blue shift in the exciton transition. But for polymers, this blue shift is smaller than the red shift caused by planarization; hence, we see an overall red shift on going from solution to the solid film. However, it is still difficult to explain why there are more than one shoulder peak (at least two peaks for P3HT at around 565 and 605 nm respectively), and the red shifts of the two shoulder peaks as compared with the “solid-state monomer peaks” at around 525 nm (this peak exists for all solid films studied here). Davydov splitting theory seems not very applicable here, because it means that the planar polymers in solid film would show *distinct* structure change as compared with their aggregation states with the effective conjugation length being *much longer* during the self assembly processes.

According to the peak separation results (Fig. 6), we suggest that the vibronic progression is the main reason for these “fine structures” in RR-P3HT films (and other regioregular conjugated polymers). When aggregation forms, there is an obvious narrowing of the main peak at around 525 nm, which means that, a fixing of the polymer conformation in solids leads to decrease of number of the energetic states and simplify the UV spectra. In another word, aggregation with the π - π stacking interaction assists the planarization of the polymer backbones and narrow the absorption peak. In this case, fine vibronic structures can be resolved as additional peaks or shoulders. With a more careful peak separation for the UV-vis absorption spectra of drop-cast P3HT film, a small peak at 521 nm appears and it is mathematically stable with improved fitting reliability as compared with the former results. Three peaks at 521, 564, and 609 nm form a perfect vibronic progression. P3HT polymer, the vibronic progression is due to the in-plane ring breathing mode at around 1400 cm^{-1} , and it coincides well with the peak separation results. According to Spano’s model [39], this vibronic progression also means a weak exciton coupling in H-aggregates of polymers with lamellar structure. In fact, the aggregation states of RR-P3HT are very complex and are not fully understood yet.

4. Conclusions

We have successfully fabricated low-cost OFETs with soluble and crosslinkable poly (4-vinylphenol) (PVP) as the gate insulator and poly (3-hexylthiophene) (P3HT) as the active semiconductor on glass or PEN substrate. Low-cost drop-casting and spin-coating were employed to obtain organic thin films with controlled thickness and different morphology. As a comparison, OFETs with vacuum deposited pentacene film and polycarbonate (PC) gate insulator were also fabricated and investigated. We get the following conclusion. Aggregation

states and charge transfer mechanisms in the P3HT films were studied in OFETs. Both regioregular and regiorandom P3HT (RRa-P3HT) were studied and also the oligomer acenes of pentacene. Pentacene films were deposited by the physical vapor deposition (PVD) method on the gate insulator of PC. RRa-P3HT films showed mobilities one or two orders lower than those of RR-P3HT films because they were amorphous in both spin-coated and drop-cast films. Experimental results also revealed a correlation between the mobility and the aggregation states that the larger aggregate size and number can result in the higher mobility. Pentacene films (in herringbone structure) displayed mobilities about two orders higher than RR-P3HT (in lamellar structure), because it formed on polycrystalline films with crystal size being much larger than those in RR-P3HT semicrystalline films. For RR-P3HT films, aggregation with the π - π stacking interaction was found to assist the planarization of the polymer backbones, however, the alkyl side-chain interactions could result in chain folding within one polymer, and hence decrease the crystallinity and mobility greatly. Multiple π - π^* absorption peaks for RR-P3HT thin films were ascribed to the vibronic progression with the in-plane ring breathing mode assisted by polymer aggregation but not to the typical Davydov splitting; and this explanation coincide well with the relatively poor crystallinities and low mobilities in semicrystalline P3HT thin films.

These results imply that there are still many spaces to increase the mobility of π -conjugated polymer films if larger π - π stacked crystal size can be obtained. The performances of the OFETs can be further improved by optimizing the structure and morphology of organic semiconductor film, the properties of the gate insulator layer, and the configuration of the OFETs. For real applications of all-polymer transistors, their stability should also be enhanced. Insertion of an isolation layer or a vacuum package is recommended to prevent ambient humidity, oxygen, and unintended doping.

Acknowledgements

The present work was partly supported by a grant of the Frontier Research Project (Continuation) “Materials for the 21st Century – Development of a Novel Device Based on Fundamental Research into Materials Development for the Environment, Energy and Information –” (for fiscal years 2007–2009) from the Ministry of Education, Culture, Sports, Science and Technology of Japan.

References

- [1] R. H. Friend, R. W. Gymer, A. B. Holmes, J. H. Burroughes, R. N. Marks, C. Taliani, D. C. C. Bradley, D. A. Dos Santos, J. L. Bredas, M. Logdlund, W. R. Salaneck, *Nature* **397** (1999) p.121.
- [2] H. Sirringhaus, N. Tessler, R. H. Friend, *Science* **280** (1998) p.1741.
- [3] C. D. Dimitrakopoulos, S. Purushothaman, I. Kymissis, A. Callegair, J. M. Shaw, *Science* **283** (1999) p.822.
- [4] B. Crone, A. Dodabalapur, Y.-Y. Lin, R. W. Filas, Z. Bao, A. LaDuca, R. Sarpeshkar, H. E. Katz, W. Li, *Nature* **403** (2000) p.521.
- [5] M. Angelopoulos, *IBM J. Res. & Dev.* **45** (2001) p.57.
- [6] H. Shirakawa, E. J. Louis, A. G. MacDiarmid, C. K. Chiang, A. J. Heeger, *J. Chem. Soc. Chem. Commun.* (1977) p.578.
- [7] T. Skotheim, (Ed.), *Handbook of Conducting Polymers*, vols. 1 and 2, Marcel Dekker Inc., New York, 1986.
- [8] G. H. Gelinck, T. C. T. Geuns, D. W. De Leeuw, *Appl. Phys. Lett.* **77** (2000) p.1487.
- [9] B. Crone, A. Dodabalapur, R. Sarpeshkar, A. Gelperin, H. E. Katz, Z. Bao, *J. Appl. Phys.* **91** (2002) p.10140.

- [10] W. Riess, H. Riel, T. Beierlein, W. Brutting, P. Muller, P. F. Seidler, *IBM J. Res. & Dev.* **45** (2001) p.77.
- [11] R. H. Friend, J. H. Burroughes, T. Shimoda, *Phys. World (UK)* **12** (1999) p.35.
- [12] J. H. Schon, C. Kloc, B. Batlogg, *Org. Electron.* **1** (2000) p.57.
- [13] N. Karl, J. Marktanner, R. Stehle, W. Warta, *Synth. Met.* **41-43** (1991) p.2473.
- [14] J. H. Schon, C. Kloc, B. Batlogg, *Science* **288** (2000) p.2338.
- [15] V. C. Sundar, J. Zaumseil, V. Podzorov, E. Menard, R. L. Willett, T. Someya, M. E. Gershenson, J. A. Rogers, *Science* **303** (2004) p.1644.
- [16] J. H. Schon, B. Batlogg, *J. Appl. Phys.* **89** (2001) p.336.
- [17] M. Pope, C. E. Swenberg, *Electronic Processes in Organic Crystals and Polymers*, Oxford University Press, Oxford, 1999, p.337.
- [18] G. Horowitz, *Adv. Mater.* **10** (1998) p.3.
- [19] R. Cugola, U. Giovanella, P. Di Gianvincenzo, F. Bertini, M. Catellani, S. Luzzati, *Thin Solid Films* **511-512** (2006) p.489.
- [20] H. Yang, T. J. Shin, L. Yang, K. Cho, C. Y. Ryu, Z. Bao, *Adv. Funct. Mater.* **15** (2005) p.671.
- [21] R. J. Kline, M. D. McGehee, M. F. Toney, *Nature Mater.* **5** (2006) p.222.
- [22] H. Sirringhaus, P. J. Brown, R. H. Friend, M. M. Nielsen, K. Bechgaard, B. M. W. Langeveld-Voss, A. J. H. Spiering, R. A. J. Janssen, E. W. Meijer, P. Herwig, D. M. de Leeuw, *Nature* **401** (1999) p.685.
- [23] T. Miteva, L. Palmer, L. Kloppenburg, D. Neher, U. H. F. Bunz, *Macromolecules* **33** (2000) p.652.
- [24] J. K. Politis, J. C. Nemes, M. D. Curtis, *J. Am. Chem. Soc.* **123** (2001) p.2537.
- [25] A. Koren, M. D. Curtis, A. H. Francis, J. W. Kampf, *J. Am. Chem. Soc.* **125** (2003) p.5040.
- [26] F. C. Spano, S. Siddiqui, *Chem. Phys. Lett.* **314** (1999) p.481.
- [27] N. DiCesare, M. Belletete, C. Marrano, M. Leclerc, G. Durocher, *J. Phys. Chem.* **103** (1999) p.795.
- [28] N. DiCesare, M. Belletete, M. Leclerc, G. Durocher, *J. Phys. Chem.* **103** (1999) p.803.
- [29] F. C. Spano, *J. Chem. Phys.* **122** (2005) 234701.
- [30] F. C. Spano, *Annu. Rev. Phys. Chem.* **57** (2006) p.217.
- [32] M.D. Curtis, *Macromolecules* **34** (2001) p.7905.
- [33] M. Halik, H. Klauk, U. Zschieschang, G. Schmid, S. Poomarenko, S. Kirchmeyer, W. Weber, *Adv. Mater.* **15** (2003) p.917.
- [34] R. J. Kline, M. D. McGehee, E. N. Kadnikova, J.-S. Liu, J. M. J. Frechet, and M. F. Toney, *Macromolecules* **38** (2005) p.3312.